Available online at www.sciencedirect.com

SCIENCE DIRECT®

Nuclear Medicine and Biology 32 (2005) 673–678

NUCLEAR MEDICINE — AND — BIOLOGY

www.elsevier.com/locate/nucmedbio

Mass effect of injected dose in small rodent imaging by SPECT and PET

Mei-Ping Kung[a], Hank F. Kung[a,b,*]

[a]*Department of Radiology, University of Pennsylvania, Philadelphia, PA 19104, USA*
[b]*Department of Pharmacology, University of Pennsylvania, Philadelphia, PA 19104, USA*

Received 22 February 2005; received in revised form 2 April 2005; accepted 2 April 2005

Abstract

This paper discusses the effect of mass (chemical quantity) of injected dose on positron emission tomography (PET) and single-photon emission computed tomography (SPECT). Commonly, PET or SPECT imaging study uses a "no-carrier added" dose, which contains a small amount of radioactive imaging agent (in picogram to microgram). For small animal (rodent) imaging studies, specifically targeting binding sites or biological processes, the mass (chemical quantity) in the dose may significantly modify the binding, pharmacokinetics and, ultimately, the imaging outcome. Due to differences in size and other physiological factors between humans and rodents, there is a dramatic divergence of mass effect between small animal and human imaging study. In small animal imaging studies, the mass, or effective dose (ED_{50}), a dose required for 50% of receptor or binding site occupancy, is usually not directly related to binding potential (B_{max}/K_d) (measured by in vitro binding assay). It is likely that dynamic interplays between specific and nonspecific binding in blood circulation, transient lung retention, kidney excretion, liver–gallbladder flow, soft tissue retention as well as metabolism could each play a significant role in determining the concentration of the tracer in the target regions. When using small animal imaging for studying drug occupancy (either by a pretreatment, coinjection or chasing dose), the mass effects on imaging outcome are important factors for consideration.

Keywords: Molecular imaging; Receptor binding; Specific activity and small animal imaging

1. Introduction

Gamma emitting radioactive imaging agents (radiolabeled tracers), commonly used for positron emission tomography (PET) and single-photon emission computed tomography (SPECT) targeting receptors or specific binding sites, are prepared in a high specific activity. In human imaging studies, only a small chemical amount of tracer is injected (in a range of picogram to microgram). This tracer dose has several advantages, including conforming to true tracer kinetics and giving a lower or negligible toxicity. Recent advances in small animal imaging with the same human tracers have led to a burgeoning of efforts in applying these imaging agents targeting receptors or specific binding sites or enzymatic reactions in small animals (rodents including rats and mice) [1–12]. Small rodent imaging quantitatively accesses the status of gene expression, including the number of receptors or specific binding sites, in the same animal by repeating imaging studies. This approach may reduce the individual differences and provide longitudinal information on the receptor or specific binding sites in the same animal. The SPECT or PET imaging of rodents is useful to examine macro changes in relation to the uptake and retention due to the presence of specific receptors or binding sites in the whole volume of tissues or organs. Quantitative evaluation of specific binding sites

Abbreviations: ADAM, (SERT ligand) 2-[(2-amino-4-iodophenyl)thio]-*N*,*N*-dimethyl-benzenemethanamine, [305352-10-7]; CFT, (DAT ligand) 3-[4-(fluoro-^{18}F)phenyl]-8-methyl-, 8-azabicyclo[3.2.1]octane-2-carboxylic acid, methyl ester, (1*R*,2*S*,3*S*,5*S*)-(WIN35428) [178693-47-5]; DAT, dopamine transporter; DASB, (SERT ligand) 3-amino-4-(2-dimethylaminomethylphenylsulfanyl)benzonitrile; ECD, [^{99m}Tc]-ethyl cysteinate dimer; FDG, 2-fluoro-2-deoxy-D-glucose; HMPAO, [^{99m}Tc]-D,L-hexamethylpropylene amine oxime; IBZM, (dopamine D_2/D_3 receptor ligand) *N*-[[(2*S*)-1-ethyl-2-pyrrolidinyl]methyl]-2-hydroxy-3-iodo-6-methoxy-benzamide [84226-06-2]; IMP Iofetamine, *N*-isopropyl-*p*-iodoamphetamine; 6-Fluoro-DOPA, 2-Fluoro-5-hydroxy-L-tyrosine; IMPY, 6-iodo-2-(4′-dimethylamino-)phenyl-imidazo[1,2]pyridine; Raclopride, 3,5-dichloro-*N*-[[(2*S*)-1-ethyl-2-pyrrolidinyl]methyl]-2-hydroxy-6-methoxy-benzamide [84225-95-6] (dopamine D_2/D_3 receptor ligand); SERT, serotonin transporter; WAY100635, (5-HT1A ligand) *N*-[2-[4-(2-methoxyphenyl)-1-piperazinyl] ethyl]-*N*-2-pyridinyl-cyclohexanecarboxamide, [146714-97-8].

* Corresponding author. Department of Radiology, University of Pennsylvania, Philadelphia, PA 19104, USA. Tel.: +1 215 662 3096; fax: +1 215 349 5035.

E-mail address: kunghf@sunmac.spect.upenn.edu (H.F. Kung).

0969-8051/$ – see front matter © 2005 Elsevier Inc. All rights reserved.
doi:10.1016/j.nucmedbio.2005.04.002

in vivo is often difficult to assess by other imaging techniques. Recently, many transgenic models have been developed in mice or rats as animal models for various human diseases. Imaging of these rodents can provide a method for testing changes of specific receptors or binding sites in the animals after genetic manipulations without autopsy. Theoretically, by repeated imaging studies in the same animal we can reduce the total number of animals for a study [3,13]. To fully explore the feasibility of small animal imaging studies of limited binding sites, careful consideration of the effect of total chemical quantity (mass) in the injected dose is very important for the success of imaging outcome.

2. Three types of uptake and retention mechanisms

Generally, there are three types of mechanisms of uptake and retention of radiopharmaceuticals [13]: (1) nonsaturable binding (examples: [^{18}F]fluoride for active bone surface uptake [14] [^{15}O]water, [^{123}I]IMP, [^{99m}Tc]ECD and [^{99m}Tc]HMPAO for regional cerebral perfusion study [15]), (2) intermediate saturable binding sites (examples: [^{18}F]6-fluoro-metatyrosine [16] or [^{18}F]6-fluoro-DOPA [17] measuring aromatic amino acid decarboxylase and [^{18}F]FDG measuring glucose transporter and hexokinase [18,19]), (3) saturable binding sites (examples: [^{11}C]raclopride [20,21] and [^{123}I]IBZM [22,23] for dopamine D_2/D_3 receptors; [^{11}C]DASB [24,25] and [^{123}I]ADAM [26,27] for serotonin transporters; [^{123}I]IMPY for imaging β-amyloid plaques [28,29] and [^{111}In]Octreotide for imaging somatostatin receptors [30]). This paper will focus on the mass effect on imaging of saturable binding sites. Special emphasis will be on the mass effect of imaging dopamine D_2/D_3 receptors and serotonin transporters in the rat brain.

For imaging saturable binding sites, an extra amount of "carrier" is often added in vivo to study the "saturability" of binding sites by the extra mass. Presumably, the presence of the extra chemical mass will compete and eventually overwhelm, or saturate, the binding sites. By using escalating "carrier-added" doses, the effective dose (ED_{50}), which blocks 50% of specific binding, can be estimated (Fig. 1). The results demonstrate that the number of binding sites is limited. The competition between the "hot" and the "cold" compounds provides further evidence that the binding to the target sites is saturable and highly specific. As such, the ED_{50} value is related to the binding potential (B_{max}/K_d) of target sites. However, in vivo experiments appear not to reflect a direct relationship; the binding potential is not a good predictor of ED_{50} value. The K_d and B_{max} values measured by in vitro equilibrium binding assays are not useful to predict dynamic in vivo saturation experiments (ED_{50} value) in living animals, because of other physiological factors, such as in vivo metabolism (which is mass dependent), in vivo nonspecific binding and excretion in the blood, lungs, kidneys and other tissues or organs. The K_d and B_{max} values measured by in vivo imaging in rodents are often expressed as "apparent" K_d and B_{max} values; this is a reflection of differences between in vitro and in vivo measurements [31].

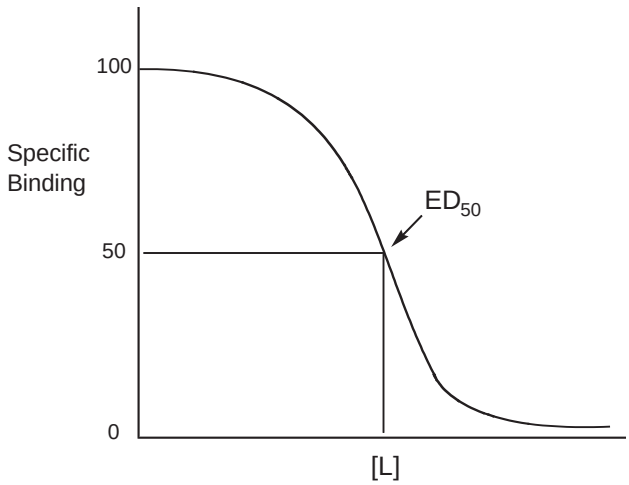

Fig. 1. Saturation of specific binding sites by carrier-added ligand [L] can be defined by the ligand concentration, which reduces the specific binding signal by 50% (ED_{50}). The specific binding can be determined by escalating carrier doses and using either ex vivo dissection techniques, or in vivo small animal imaging with PET or SPECT.

3. Small animal vs. human — differences in size and dose

It has been reported previously [13,32] that the average weight of humans vs. rats is 70 kg vs. 250 g (a ratio of 280). Due to the different sizes of human head and rat head, 18 vs. 3 cm, there is a difference in attenuation by a factor of 0.3. The net difference in obtaining the same PET signal is about $280 \times 0.3 = 84$ [13]. This factor may be slightly different for SPECT, because the gamma ray energies for single photon radionuclides are usually lower. It is important to note that this factor based on body weight and physical decay is often not linearly related to imaging outcome (the actual count rate in the brain). Frequently, in order to obtain sufficient count rates in the target areas, such as in the brain, doses close to those in human imaging studies are injected, and the effect of mass (a higher dose based on mCi/kg body weight) on rodent imaging study has been evaluated and discussed [13,20,32–34]. Previously, [^{11}C]raclopride was evaluated in rat brain using microPET imaging [20,31]. The relative size and doses for [^{11}C]raclopride imaging studies in humans, rats and mice are summarized in Table 1.

In Table 1B, it was demonstrated that if a normal human receives a 10-mCi dose of [^{11}C]raclopride (at the time of injection), if the specific activity of the preparation is 1000 Ci/mmol, then the receptor occupancy will be below 1%, a very low occupancy [20,32]. However, if the same study is performed in rats and only 1 mCi is injected (same specific activity), the amount of dose will be

Table 1
Examples on the estimation of size and dose of [^{11}C]raclopride (at the time of injection) used in PET imaging

A. Estimated size of brain, striatum, midbrain and cerebellum in different species

	Body weight	Brain weight	Striatum weight	Dopamine D_2/D_3 receptor[a]
Human	70 kg	1.5 kg	40 g	13.6 nmol/kg
Rats	250 g	1.5 g	0.05 g	19.8 nmol/kg
Mice	25 g	0.4 g	0.03 g	20 nmol/kg

B. Injected doses for [^{11}C]raclopride (the occupancy of a binding can be estimated by Activity/(SpecificActivity*Wt)=ED_{50}*Occ/(1−Occ); for raclopride ED_{50}=17.1 nmol/kg; modified from Hume et al [32])

	Dose	Specific activity	% Occupancy
Human	10 mCi	1000 Ci/mmol 1 μCi=1 pmol	<1
Rats	1 mCi	1000 Ci/mmol	19
Mice	1 mCi	1000 Ci/mmol	70

[a] Receptor density in striatum.

sufficient to occupy 19% of the receptor. Apparently, the occupancy of the receptor site is significant under this condition; a slight increase in the dose or a decrease in the specific activity will dramatically induce changes in physiology, such as dyskinesia (usually observed when more than 50% of the dopamine D_2/D_3 receptors are saturated). The mass effect of injected dose of [^{11}C]raclopride in rats was obtained by microPET imaging studies. It is estimated that a 50% occupancy was observed at a dose of 17.1 nmol/kg body weight [31]. At a tracer level (<1.5 nmol/kg), the distribution volume ratio (DVR) of striatum dopamine D_2/D_3 receptors measured by microPET imaging was 2.43. When the chemical dose was increased to 1.6–3.7 nmol/kg (the injected dose was 0.16–0.5 mCi with a range of specific activity of 70–770 Ci/mmol), the DVR was 2.08, suggesting a 9–18% occupancy [20]. Using a similar calculation for [^{11}C]raclopride imaging study in mice, it is estimated that the same 1 mCi of [^{11}C]raclopride will lead to a 70% dopamine D_2/D_3 receptor occupancy in the brain. At this level of occupancy of dopamine receptors dyskinesia will occur. Significantly, microPET imaging study of the dopamine receptor in the striatum of a mouse may only be suitable when there is a 10-fold increase in the specific activity or a 10-fold reduction of the injected dose.

Using the values listed in Table 2, there is a 0.12% uptake in the striatum at 30 min post-intravenous injection, then one can estimate the concentration of raclopride in the striatum of a 250-g rat: 17.1 nmol/kg×0.25 kg/g×0.0012=5.1 pmol/kg (Table 2) [35]. It was reported that using in vitro binding assay and [^{3}H]raclopride, the B_{max} for the striatum of rat and human brain was 19.8 and 13.6 fmol/mg protein [35]. If we assume that wet striatum tissue contains 10% protein, then the total number of dopamine D_2/D_3 binding sites (B_{max}) in the rat striatum is (19.8×0.1)=1.98 fmol/mg wet tissue=1.98 nmol/kg. This concentration of raclopride in the rat striatum is not the same as the concentration estimated by using the ED_{50} value estimated in vivo (5.1 pmol/kg; Table 2), because factors such as nonspecific binding, in vivo metabolism and excretion from other organs or tissues will affect the availability of the tracer binding to the target sites.

It was reported previously (Tables 2 and 3) that the occupancy of binding sites can be estimated by Activity/SpecificActivity*Wt=ED_{50}*Occ/(1−Occ) [32]. If the saturating dose (ED_{50}) of a binding site is known and the specific activity is also measured, it will be feasible to use this simple equation to estimate the potential of saturation of binding sites. This pharmacological constraint reported previously is the result of association between binding affinity ED_{50} and total number of binding sites. It is important to estimate the potential of pitfalls in receptor or binding site occupancy prior to microPET or microSPECT imaging study in rodents [32].

In addition, injecting a human dose to small rodents will lead to a high-radiation dose to the animal. The high-radiation dose to the small animals may be a confounding factor, which could change physiology and lead to invalid

Table 2
Comparison of K_d vs. ED_{50} for dopamine D_2/D_3 receptors and serotonin transporters (SERT) in the rat brain

Ligand	Binding site	In vitro binding			In vivo		
		K_d (nM)	B_{max} (nM)	B_{max}/K_d	ED_{50} (iv) (nmol/kg)	Estimated concentration (pmol/kg)[a]	Ref.
[$^{123/125}$I]IBZM[b]	D_2/D_3	0.4	48	120	37	23[b]	[36,37]
[$^{123/125}$I]ADAM[c]	SERT	0.15	19.4	129	60	66[c]	[26]
[^{11}C]/[^{3}H] raclopride[d]	D_2/D_3	1.0	19.8	19.8	17.1	5.1[d]	[20,32,38]
[^{11}C]DASB[e]	SERT	0.1[f]	19.4[g]	194	56	61.6	[39]

[a] Estimated concentration values are calculated based on ED_{50} (iv)×0.25 kg (body wt)×% dose/g.
[b] IBZM: at 30 min, 0.25 % dose/g in striatum (0.05 g); for IBZM the estimated concentration is equal to 37 nmol/kg (ED_{50})×0.25 kg (body wt)×0.25%/g (uptake in striatum at 30 min)=23 pmol/kg.
[c] ADAM: at 120 min, 0.44%/g in midbrain.
[d] Raclopride: 60 min, 0.12%/g in striatum.
[e] DASB: 60 min, 0.62%/g in midbrain (0.03 g).
[f] K_i values reported by Wilson et al. [25,39].
[g] Estimated by using [^{125}I]ADAM.

Table 3
Pharmacological constraints (1% occupancy) of various C-11 tracers from human to mice (modified from Hume et al. [32])

Compounds (target sites)	K_d (nM)	ED_{50} (nmol/kg)	Man (70 kg) (mCi)	Rat (0.3 kg) (mCi)	Mouse (0.02 kg) (mCi)
[^{11}C]CFT (DAT)	10	242	459	2	0.13
[^{11}C]raclopride (D_2/D_3)	1.0	17.1	32	0.14	0.04
[^{11}C]WAY100635 (5-HT1A)	0.1	4.8	9	0.04	0.003

Specific activity of C-11 tracers: 100 MBq/nmol (3000 Ci/mmol); Activity/SpecificActivity*Wt=ED_{50}*Occ/(1−Occ) (see Ref. [32]).

results of imaging study. The high-radiation dose may also prevent multiple studies in the same animal [40].

4. Carrier-added biodistribution studies

Titration of a limited number of binding sites by a massive amount of "carrier" is based on in vivo competition of "cold" ligand against the "hot" ligand for the same binding sites. In theory, the "hot" and "cold" ligand should have the same biodistribution in vivo; therefore, it is possible to use the tracer kinetic model as measured by in vivo imaging or ex vivo dissection techniques to measure the in vivo competition. Compared to the binding capacity (B_{max} value obtained by in vitro binding assay), the amount of chemical mass required to saturate the in vivo binding is not as expected (the dose in the target areas of the brain is estimated based on the tracer biodistribution data). The discrepancy may be caused by many physical or biological factors. The quantitation of images based on positron decays (511 keV) or single photons is not absolute. Physical properties of scattering and attenuation of gamma emission will lead to errors in estimating the counts in target and nontarget areas [11,20]. The anesthesia commonly used for immobilizing the rodents will also have significant physiological effects [41–47]. When "cold" carrier is added in the injected dose, it is possible that the kinetics of in vivo biodistribution may change. There are many factors that may affect the biodistribution. There are nonspecific binding sites in plasma, which may have significant effect on the availability of the tracer in the blood circulation. Initial lung uptake and washout may be affected by nonspecific binding, and when the nonspecific binding sites are "saturated," the additional dose will pass through the lungs with higher efficiency. The metabolism in peripheral tissues, mainly in the liver or other tissues or organs, could be different; especially, the amount of carrier may affect the enzyme kinetics and thus the rate of degradation, which leads to differences in bioavailability. The kidneys normally will filter out "foreign" material from the blood circulation; the filtering process in the kidneys, either by specific or nonspecific transporters, is likely to be dependent on the carrier dose in the blood circulation. Therefore, changing the carrier amount in the injected dose will likely change the kidney excretion and the results of imaging study. It is likely that the dose response due to factors listed above is not linear. The mass effects of injected dose on imaging studies will not be entirely correlated with the binding constant obtained by in vitro equilibrium binding assay.

5. Drug occupancy studies

There are different approaches in studying the effect of mass, by using "cold" carrier or competing drugs (sometimes referred as pseudo-carriers) [21,32,34,48,49]: (1) pretreatment study — usually a larger chemical dose is injected prior to the injection of a radioactive tracer dose. Presumably, pretreatment of the injected "cold" carrier or another drug competing for the same binding site can reach the target sites prior to the arrival of the labeled tracer. In this type of study, the tracer will likely compete less with the nonspecific binding sites in the peripheral tissues. (2) Coinjection study—the radioactive tracer dose is premixed with "carrier," i.e., nonradioactive larger chemical amount. (3) Chasing study—nonradioactive chemical dose is injected after the tracer dose has been injected. Usually, the tracer dose is injected first allowing time for the tracer distribution to reach an equilibrium or semi-equilibrium state, after which the chemical "chasing dose" is injected to compete with the specific binding at the equilibrium state. Adding the carrier (or pseudo-carrier) for the competition studies will likely be strongly influenced by the mass effect.

The effect of mass of injected dose on the specific uptake in rats or mice for [^{111}In]pentetreotide/pentetreotide is shown in Table 4. Endocrine tumors that overexpress somatostatin receptors can be imaged by [^{111}In]pentetreotide

Table 4
Effects of varying mass of pentetreotide on the uptake of [^{111}In]pentetreotide in the octreotide receptor positive organs of rats (modified from Ref. [30])

Mass (μg)	Specific activity (mCi/μg)	Pancreas (% dose/g)	Pituitary (% dose/g)	Adrenals (% dose/g)
0.02	4.05	1.0	0.5	1.5
0.1	0.81	1.4	0.6	3.5
0.5	0.16	2.0	1.0	5.5
5.0	0.016	3.0	0.8	5.0
50	0.0016	1.0	0.3	4.0

Table 5
Effect of "carrier" IMPY on organ uptakes of [^{125}I]IMPY in TT mice (modified from Ref. [29])

Mass IMPY (mg/kg)	Specific activity (Ci/mmol)	Blood (% dose/organ) 2 min/30 min	Brain (% dose/organ) 2 min/30 min
0	2200	6.46/5.89	1.94/0.52
2	0.44	7.20/3.93	2.72/0.44
10	0.088	8.48/4.92	3.86/0.56

Values are presented as the average of three double transgenic (TT) mice in each point.

(OctreoScan). When [^{111}In]pentetreotide was injected into rats with varying amounts of "cold" pentetreotide at 24 h after the intravenous injection, the expected uptake in the endocrine organs, such as pancreas, pituitary and adrenals containing somatostatin receptors, displayed dramatic changes (Table 4). In the targeted organs, there is a bell-shape relationship between the uptake and the carrier dose, suggesting that there may be low-affinity and high-capacity nonspecific binding sites, and the mass effect of injected dose is not linear.

Another interesting example is the mass effect on the biodistribution of [^{125}I]IMPY, a potential tracer for detecting β-amyloid plaques, Aβ protein aggregates appear to be associated with Alzheimer's disease [29,50]. A suitable method for testing the localization of the β-amyloid plaques (abnormal protein aggregates) in the brain is by performing biodistribution study in transgenic animals specially engineered to produce excessive amounts of Aβ plaques in the brain. One such genetically modified mouse is PS1/APP mice, which produce an excess amount of Aβ protein aggregates in the brain within 12 months. When [^{125}I]IMPY was injected into these transgenic mice at escalating doses, the biodistribution showed a dramatic change (Table 5). There was a significant increase in the brain uptake with increasing amount of coinjected IMPY [29]. Taken together, these findings suggest that IMPY is metabolized in the peripheral tissues, and adding the carrier appears to slow down the degradation, thus allowing more [^{125}I]IMPY to be delivered into the brain of transgenic mice (Table 5). Consistently, carrier IMPY significantly ($P<.05$) increased the amount of [125I]IMPY in the plasma at the early time point (at 2 min).

6. Summary

Specific target-binding sites are important for human physiology as well as molecular targets for drug development. It is likely that small animal imaging for these targets will play an important role in the future for developing new imaging agents and new drugs for therapeutic applications. Molecular imaging of changes at the gene level in rodents may be assessed to improve our understanding of human diseases. Many potential physical and biological pitfalls related to the effects of mass (carrier dose) need to be considered and addressed carefully before the small animal imaging techniques can be effectively applied in molecular imaging and in assisting future drug development.

References

[1] Acton PD, Kung HF. Small animal imaging with high resolution single photon emission tomography. Nucl Med Biol 2003;30:889–95.

[2] Rowland DJ, Lewis JS, Welch MJ. Molecular imaging: the application of small animal positron emission tomography. J Cell Biochem Suppl 2002;39:110–5.

[3] Hume SP, Myers R. Dedicated small animal scanners: a new tool for drug development? Curr Pharm Des 2002;8:1497–511.

[4] Jacobs AH, Li H, Winkeler A, Hilker R, Knoess C, Ruger A, et al. PET-based molecular imaging in neuroscience. Eur J Nucl Med Mol Imaging 2003;30:1051–65.

[5] Lewis JS, Achilefu S, Garbow JR, Laforest R, Welch MJ. Small animal imaging. Current technology and perspectives for oncological imaging. Eur J Cancer 2002;38:2173–88.

[6] Myers R, Hume S. Small animal PET. Eur Neuropsychopharmacol 2002;12:545–55.

[7] Herschman HR. Micro-PET imaging and small animal models of disease. Curr Opin Immunol 2003;15:378–84.

[8] Weber S, Bauer A. Small animal PET: aspects of performance assessment. Eur J Nucl Med Mol Imaging 2004;31:1545–55.

[9] Yang Y, Tai YC, Siegel S, Newport DF, Bai B, Li Q, et al. Optimization and performance evaluation of the microPET II scanner for in vivo small-animal imaging. Phys Med Biol 2004;49:2527–45.

[10] Chatziioannou AF. Molecular imaging of small animals with dedicated PET tomographs. Eur J Nucl Med Mol Imaging 2002; 29:98–114.

[11] Fahey FH, Gage HD, Buchheimer N, Smith HC, Harkness BA, Williams RC, et al. Evaluation of the quantitative capability of a high-resolution positron emission tomography scanner for small animal imaging. J Comput Assist Tomogr 2004;28:842–8.

[12] Cherry SR. In vivo molecular and genomic imaging: new challenges for imaging physics. Phys Med Biol 2004;49:R13–R48.

[13] Jagoda EM, Vaquero JJ, Seidel J, Green MV, Eckelman WC. Experiment assessment of mass effects in the rat: implications for small animal PET imaging. Nucl Med Biol 2004;31:771–9.

[14] Hetzel M, Arslandemir C, Konig HH, Buck AK, Nussle K, Glatting G, et al. F-18 NaF PET for detection of bone metastases in lung cancer: accuracy, cost-effectiveness, and impact on patient management. J Bone Miner Res 2003;18:2206–14.

[15] Matsuda H, Li YM, Higashi S, Sumiya H, Tsuji S, Kinuya K, et al. Comparative SPECT study of stroke using Tc-99m ECD, I-123 IMP, and Tc-99m HMPAO. Clin Nucl Med 1993;18:754–8.

[16] DeJesus OT, Endres CJ, Shelton SE, Nickles RJ, Holden JE. Evaluation of fluorinated m-tyrosine analogs as PET imaging agents of dopamine nerve terminals: comparison with 6-fluoroDOPA. J Nucl Med 1997;38:630–6.

[17] Whone AL, Bailey DL, Remy P, Pavese N, Brooks DJ. A technique for standardized central analysis of 6-(18)F-fluoro-L-DOPA PET data from a multicenter study. J Nucl Med 2004;45:1135–45.

[18] Waki A, Fujibayashi Y, Yonekura Y, Sadato N, Ishii Y, Yokoyama A. Reassessment of FDG uptake in tumor cells: high FDG uptake as a reflection of oxygen-independent glycolysis dominant energy production. Nucl Med Biol 1997;24:665–70.

[19] Pauwels EK, Ribeiro MJ, Stoot JH, McCready VR, Bourguignon M, Maziere B. FDG accumulation and tumor biology. Nucl Med Biol 1998;25:317–22.

[20] Alexoff DL, Vaska P, Marsteller D, Gerasimov T, Li J, Logan J, et al. Reproducibility of ^{11}C-raclopride binding in the rat brain measured with the microPET R4: effects of scatter correction and tracer specific activity. J Nucl Med 2003;44:815–22.

[21] Ginovart N, Sun W, Wilson AA, Houle S, Kapur S. Quantitative validation of an intracerebral beta-sensitive microprobe system to determine in vivo drug-induced receptor occupancy using [^{11}C]raclopride in rats. Synapse 2004;52:89–99.

[22] Scherfler C, Scholz SW, Donnemiller E, Decristoforo C, Oberladstatter M, Stefanova N, et al. Evaluation of [(123)I]IBZM pinhole SPECT for the detection of striatal dopamine D(2) receptor availability in rats. Neuroimage 2005;24:822–31.

[23] Kung HF, Billings JJ, Guo Y-Z, Xu X, Mach RH, Blau M, et al. Preparation and biodistribution of [^{125}I]IBZM: a potential CNS D_2 dopamine receptor imaging agent. Int J Radiat Appl Instrum, B Nucl Med Biol 1988;15:195–201.

[24] Meyer JH, Houle S, Sagrati S, Carella A, Hussey DF, Ginovart N, et al. Brain serotonin transporter binding potential measured with carbon 11-labeled DASB positron emission tomography: effects of major

depressive episodes and severity of dysfunctional attitudes. Arch Gen Psychiatry 2004;61:1271–9.

[25] Wilson AA, Ginovart N, Hussey D, Meyer J, Houle S. In vitro and in vivo characterisation of [^{11}C]-DASB: a probe for in vivo measurements of the serotonin transporter by positron emission tomography. Nucl Med Biol 2002;29:509–15.

[26] Choi SR, Hou C, Oya S, Mu M, Kung MP, Siciliano M, et al. Selective in vitro and in vivo binding of [^{125}I]ADAM to serotonin transporters in rat brain. Synapse 2000;38:403–12.

[27] Oya S, Choi SR, Hou C, Mu M, Kung MP, Acton PD, et al. 2-((2-((Dimethylamino)methyl)phenyl)thio)-5-iodophenylamine (ADAM): an improved serotonin transporter ligand. Nucl Med Biol 2000; 27:249–54.

[28] Kung M-P, Hou C, Zhuang Z-P, Skovronsky D, Kung HF. Binding of two potential imaging agents targeting amyloid plaques in postmortem brain tissues of patients with Alzheimer's disease. Brain Res 2004;1025:89–105.

[29] Kung M-P, Hou C, Zhuang Z-P, Cross AJ, Maier DL, Kung HF. Characterization of IMPY as a potential imaging agent for β-amyloid plaques in double transgenic PSAPP mice. Eur J Nucl Med Mol Imaging 2004;31:1136–45.

[30] Breeman WA, Kwekkeboom DJ, Kooij PP, Bakker WH, Hofland LJ, Visser TJ, et al. Effect of dose and specific activity on tissue distribution of indium-111-pentetreotide in rats. J Nucl Med 1995; 36:623–7.

[31] Hume SP, Opacka-Juffry J, Myers R, Ahier RG, Ashworth S, Brooks DJ, et al. Effect of L-DOPA and 6-hydroxydopamine lesioning on [^{11}C]raclopride binding in rat striatum, quantified using PET. Synapse 1995;21:45–53.

[32] Hume SP, Gunn RN, Jones T. Pharmacological constraints associated with positron emission tomographic scanning of small laboratory animals. Eur J Nucl Med 1998;25:173–6.

[33] Meikle SR, Eberl S, Fulton RR, Kassiou M, Fulham MJ. The influence of tomograph sensitivity on kinetic parameter estimation in positron emission tomography imaging studies of the rat brain. Nucl Med Biol 2000;27:617–25.

[34] Eckelman WC, Frank JA, Brechbiel M. Theory and practice of imaging saturable binding sites. Invest Radiol 2002;37:101–6.

[35] Hall H, Kohler C, Gawell L, Farde L, Sedvall G. Raclopride, a new selective ligand for the dopamine-D_2 receptors. Prog Neuro-Psychopharmacol Biol Psychiatry 1988;12:559–68.

[36] Kung HF, Billings JJ, Guo Y-Z, Mach RH. Comparison of in vivo D_2 dopamine receptor binding of IBZM and NMSP in rat brain. Int J Radiat Appl Instrum, B Nucl Med Biol 1988;15:203–8.

[37] Kung HF, Pan S, Kung M-P, Billings JJ, Kasliwal R, Reilly J, et al. In vitro and in vivo evaluation of [^{123}I]IBZM: a potential CNS D_2 dopamine receptor imaging agent. J Nucl Med 1989;30:88–92.

[38] Hall H, Wedel I, Halldin C, Kopp J, Farde L. Comparison of the in vitro receptor binding properties of *N*-[^{3}H]methylspiperone and [^{3}H]raclopride to rat and human brain membranes. J Neurochem 1990;55:2048–57.

[39] Wilson AA, Ginovart N, Schmidt M, Meyer JH, Threlkeld PG, Houle S. Novel radiotracers for imaging the serotonin transporter by positron emission tomography: synthesis, radiosynthesis, and in vitro and ex vivo evaluation of ^{11}C-labeled 2-(phenylthio)araalkylamines. J Med Chem 2000;43:3103–10.

[40] Funk T, Sun M, Hasegawa BH. Radiation dose estimate in small animal SPECT and PET. Med Phys 2004;31:2680–6.

[41] Nader MA, Grant KA, Gage HD, Ehrenkaufer RL, Kaplan JR, Mach RH. PET imaging of dopamine D_2 receptors with [^{18}F]fluoroclebopride in monkeys: effects of isoflurane- and ketamine-induced anesthesia. Neuropsychopharmacology 1999;21:589–96.

[42] Croteau E, Benard F, Bentourkia M, Rousseau J, Paquette M, Lecomte R. Quantitative myocardial perfusion and coronary reserve in rats with ^{13}N-ammonia and small animal PET: impact of anesthesia and pharmacologic stress agents. J Nucl Med 2004;45: 1924–30.

[43] Votaw JR, Byas-Smith MG, Voll R, Halkar R, Goodman MM. Isoflurane alters the amount of dopamine transporter expressed on the plasma membrane in humans. Anesthesiology 2004;101:1128–35.

[44] Salmi E, Kaisti KK, Metsahonkala L, Oikonen V, Aalto S, Nagren K, et al. Sevoflurane and propofol increase ^{11}C-flumazenil binding to gamma-aminobutyric acid A receptors in humans. Anesth Analg 2004;99:1420–6.

[45] Momosaki S, Hatano K, Kawasumi Y, Kato T, Hosoi R, Kobayashi K, et al. Rat-PET study without anesthesia: anesthetics modify the dopamine D_1 receptor binding in rat brain. Synapse 2004;54: 207–13.

[46] Toyama H, Ichise M, Liow JS, Modell KJ, Vines DC, Esaki T, et al. Absolute quantification of regional cerebral glucose utilization in mice by ^{18}F-FDG small animal PET scanning and 2-^{14}C-DG autoradiography. J Nucl Med 2004;45:1398–405.

[47] Ma B, Sherman PS, Moskwa JE, Koeppe RA, Kilbourn MR. Sensitivity of [^{11}C]*N*-methylpyrrolidinyl benzilate ([^{11}C]NMPYB) to endogenous acetylcholine: PET imaging vs tissue sampling methods. Nucl Med Biol 2004;31:393–7.

[48] Shimoji K, Esaki T, Itoh Y, Ravasi L, Cook M, Jehle J, et al. Inhibition of [^{18}F]FP-TZTP binding by loading doses of muscarinic agonists P-TZTP or FP-TZTP in vivo is not due to agonist-induced reduction in cerebral blood flow. Synapse 2003;50:151–63.

[49] Houston GC, Hume SP, Hirani E, Goggi JL, Grasby PM. Temporal characterisation of amphetamine-induced dopamine release assessed with [^{11}C]raclopride in anaesthetised rodents. Synapse 2004;51: 206–12.

[50] Zhuang ZP, Kung MP, Wilson A, Lee CW, Plossl K, Hou C, et al. Structure–activity relationship of imidazo[1,2-*a*]pyridines as ligands for detecting beta-amyloid plaques in the brain. J Med Chem 2003;46:237–43.